

## Article

# Hydroxyl-Terminated Saponified Natural Rubber Based on the H<sub>2</sub>O<sub>2</sub>/P25-TiO<sub>2</sub> Powder/UVC-Irradiation System

Supinya Nijpanich <sup>1,2</sup>, Adun Nimpaiboon <sup>3</sup> , Pornpip Rojruthai <sup>4</sup> and Jitladda Sakdapipanich <sup>1,\*</sup>

<sup>1</sup> Department of Chemistry and Center of Excellence for Innovation in Chemistry, Faculty of Science, Mahidol University, Nakhon Pathom 73170, Thailand; supinya@slri.or.th

<sup>2</sup> Synchrotron Light Research Institute, Nakhon Ratchasima 30000, Thailand

<sup>3</sup> Rubber Technology Research Centre (RTEC), Faculty of Science, Mahidol University, Nakhon Pathom 73170, Thailand; adun.nim@mahidol.ac.th

<sup>4</sup> Division of Chemical Industrial Process and Environment, Faculty of Science, Energy and Environment, King Mongkut's University of Technology North Bangkok, Rayong 21120, Thailand; pornpip.r@sciee.kmutnb.ac.th

\* Correspondence: jitladda.sak@mahidol.ac.th

**Abstract:** Natural rubber (NR), a long-chain hydrocarbon polymer mostly consisting of *cis*-1,4-polyisoprene units, has a high molecular weight (MW) and viscosity, enabling it to show excellent physical properties. However, NR has no reactive functional group, making it difficult to react with other molecules, especially in manufacturing processes. The functionalized low-molecular-weight NR (FLNR) is a requirement to disperse ingredients into the rubber adequately. Here, the FLNR was prepared by a photochemical degradation process under UVC-irradiation in the presence of H<sub>2</sub>O<sub>2</sub> using P25-titanium oxide (TiO<sub>2</sub>) powder as a photocatalyst. The optimum condition for the preparation of FLNR was the use of 2.0 g of TiO<sub>2</sub> powder per 100 g of rubber and H<sub>2</sub>O<sub>2</sub> at 20% *w/w* under UVC-irradiation for 5 h. The hydroxyl groups were found on the NR chains due to the chain-scission of polyisoprene chains and hydroxyl radicals in the system. The weight average MW of NR decreased from 12.6 × 10<sup>5</sup> to 0.6 × 10<sup>5</sup> gmol<sup>-1</sup>, while the number average MW decreased from 3.3 × 10<sup>5</sup> to 0.1 × 10<sup>5</sup> gmol<sup>-1</sup>.

**Keywords:** natural rubber; functionalized low-molecular-weight natural rubber; photochemical degradation process; titanium oxide (TiO<sub>2</sub>)



**Citation:** Nijpanich, S.; Nimpaiboon, A.; Rojruthai, P.; Sakdapipanich, J. Hydroxyl-Terminated Saponified Natural Rubber Based on the H<sub>2</sub>O<sub>2</sub>/P25-TiO<sub>2</sub> Powder/UVC-Irradiation System. *Polymers* **2021**, *13*, 1319. <https://doi.org/10.3390/polym13081319>

Academic Editors: Dariusz M. Bieliński and Xavier Colom

Received: 3 March 2021

Accepted: 14 April 2021

Published: 17 April 2021

**Publisher's Note:** MDPI stays neutral with regard to jurisdictional claims in published maps and institutional affiliations.



**Copyright:** © 2021 by the authors. Licensee MDPI, Basel, Switzerland. This article is an open access article distributed under the terms and conditions of the Creative Commons Attribution (CC BY) license (<https://creativecommons.org/licenses/by/4.0/>).

## 1. Introduction

Natural rubber (NR) derived from the *Hevea brasiliensis* tree is a long chain hydrocarbon polymer composed of 94% *cis*-1,4-polyisoprene and 6% non-rubber components, including lipids, proteins, and inorganic constituents [1]. It has been extensively used in various applications, such as tire, medical glove, and condoms, since it provides excellent physical properties, resilience, strength, and fatigue resistance [2]. On the other hand, the very high molecular weight (MW) and hydrocarbon nature make it difficult to process and compatibilize NR with fillers or other molecules and significantly limits its chain-end usage. Several efforts to modify some NR properties by reducing its MW and introducing a certain reactive functional group at chain-ends have been reported. A shorter and functionalized NR product, called functionalized low-molecular-weight NR (FLNR), has been applied in plasticizers [3], compatibilizers [4,5], and adhesive materials [6], as well as precursors for chain extension [7–9] and grafting [10]. For instance, Isa et al. prepared the epoxidized NR in the latex state using sodium nitrite (NaNO<sub>2</sub>) as a reducing agent [11]. They found that the chain-scission of the NR chain occurred parallel with the epoxidation. Both hydroxyl and epoxide groups were observed in the degraded NR, and the degradation was influenced by temperature and reaction time. Ibrahim et al. functionalized the liquid NR via an oxidative degradation process for 24 h or 48 h [12,13]. Nevertheless, these methods require a toxic chemical and a long reaction time.

In 1988, Ravindran et al. reported the preparation of hydroxyl-terminated liquid NR via the photochemical degradation in the presence of  $\text{H}_2\text{O}_2$  under ultraviolet (UV) irradiation from a medium-pressure mercury vapor lamp and sunlight [14]. Comparing these methods, the photochemical degradation method seems more promising than other techniques due to its clean and environmentally friendly method, low in energy, and non-toxic reagent consumption.

Previously, we reported the successful preparation of functionalized styrene-butadiene rubber and skim latex by a photocatalytic degradation process using a nanometric photocatalyst in a  $\text{TiO}_2$ -film-coated Petri dish under ultraviolet irradiation [15]. The photocatalytic reaction on the  $\text{TiO}_2$  surface begins when it adsorbs light with an energy higher than its bandgap energy. The electron ( $e^-$ ) in the valence band will be excited and jump to the conduction band, leaving a positively charged hole ( $h^+$ ). When the  $e^-$  and  $h^+$  are transferred to reactive species, i.e.,  $\text{O}_2$  or  $\text{H}_2\text{O}$ , adsorbed on the  $\text{TiO}_2$  surface, the hydroxyl radicals ( $\text{OH}\cdot$ ) can be generated, as illustrated in Figure 1.

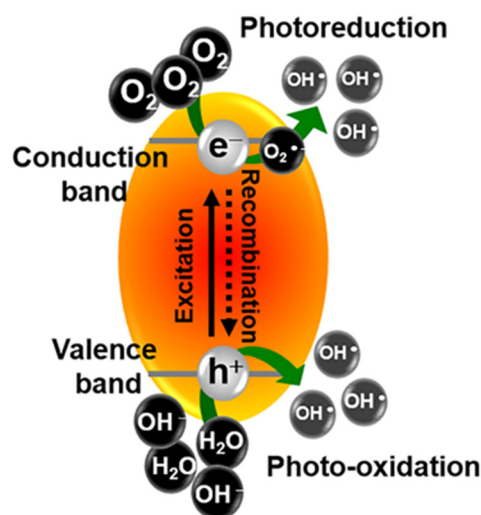


**Figure 1.** Schematic illustration of the photo-generation of charge carriers in a photocatalyst.

The generated reactive oxygen species play an important role in the decomposition of NR. It is well known that the high surface area of a photocatalyst influences its photocatalytic ability [16]. Although the FLNR could be obtained in our previous work, the reaction site was limited to the size of a Petri dish and the procedure to prepare the  $\text{TiO}_2$ -coated Petri dish was complicated. In addition, based on the NR particle structure reported by Nawamawat et al. [17], the NR particle surface was surrounded by a layer made up of proteins and phospholipids, stabilizing the hydrophobic polyisoprene chains. However, the mixed layer of phospholipids and proteins stabilized the rubber chains and obstructed the NR chains from other molecules once the photocatalytic degradation process occurred [13]. This resulted in a low reaction performance on the NR chains.

In this work, AEROXIDE<sup>®</sup> P25- $\text{TiO}_2$  powder was utilized as a photocatalyst instead of a  $\text{TiO}_2$ -coated Petri dish to enhance the reaction site due to its large specific surface area and to minimize the photocatalyst preparing step. Furthermore, a mixed layer of proteins and phospholipids surrounding the surface of NR was also preliminarily eliminated from NR particles by saponification, giving a so-called saponified NR (SPNR) latex. Then, it was used as a starting material to prepare FLNR latex in the presence of  $\text{H}_2\text{O}_2$  under UVC-irradiation using AEROXIDE<sup>®</sup> P25- $\text{TiO}_2$  powder as a photocatalyst. The optimum condition was investigated, including the effect of  $\text{TiO}_2$  powder as well as UVC-irradiation time. The prepared FLNR was further characterized using Fourier-Transform Infrared spectroscopy (FT-IR), Gel Permeation Chromatography (GPC), and Nuclear Magnetic Resonance spectroscopy (NMR).

## 2. Materials and Methods

### 2.1. Materials

The NR latex used in this study was high ammonia (HA) latex supplied from Thai rubber latex Group Public Co., Ltd. (Bang Phli District, Thailand). Hydrogen peroxide ( $\text{H}_2\text{O}_2$ , 30% *w/w*) was purchased from Merck. Methanol ( $\text{CH}_3\text{OH}$ ), sodium hydroxide (NaOH), tetrahydrofuran (THF), and toluene were purchased from Labscan<sup>®</sup>. P25-TiO<sub>2</sub> (AEROXIDE<sup>®</sup>) powder was kindly supported by Evonik industries. All chemicals are analytical (AR) grades and were used as received, without further purification.

### 2.2. Methods

#### 2.2.1. Preparation of SPNR

Prior to the saponification process, HA latex was diluted with distilled water from 60% dry rubber content (DRC) to 30% DRC in the presence of 1% *w/v* SDS. Then, latex was saponified with a 3.0% *w/v* NaOH solution [18]. The mixture was stirred at 70 °C for 3 h and cooled down at room temperature. The cream fraction was collected by double centrifugation in distilled water at 13,000 rpm (relative centrifugal force (rcf) = 15,115 × *g*) for 30 min to remove the residual lipids and proteins. Finally, the resulting latex was diluted with distilled water again to get 10% DRC of SPNR latex.

#### 2.2.2. Preparation of FLNR

The mixtures of 30 g SPNR latex at 10% DRC, TiO<sub>2</sub> powder (0, 0.25, 0.5, 1.0, 2.0 g per 100 g of rubber or phr), and H<sub>2</sub>O<sub>2</sub> (0, 5, 10, 15, 20% *w/w*) were irradiated in a self-constructed UV chamber under a 80W UV lamp ( $\lambda_{\text{max}}$  at 253 nm) for 5 h. Then, the mixtures were centrifuged at 13,000 rpm (15,115 × *g*) for 20 min to remove the TiO<sub>2</sub> particles from the solution. The cream rubber fraction was collected into a Petri dish and dried in a vacuum oven at 40 °C for 12 h. The samples were purified by dissolving in toluene and further coagulated with CH<sub>3</sub>OH. The obtained rubber was dried in a vacuum oven at 40 °C for 12 h and then subjected to the characterization.

### 2.3. Characterizations

#### 2.3.1. Determination of the Crystallinity of TiO<sub>2</sub> Powder

The AEROXIDE<sup>®</sup> P25-TiO<sub>2</sub> powder was characterized by the XRD technique using a Bruker<sup>®</sup> D8 Advance X-ray diffractometer with CuK $\alpha$  radiation ( $\lambda = 1.5406 \text{ \AA}$ ) operated at the accelerating voltage and current of 40 kV and 40 mA, respectively. The measured two theta ( $2\theta$ ) range were 20–60, with a scanning speed of 2.0 °min<sup>-1</sup>.

#### 2.3.2. Determination of the Chemical Structure of the Rubber Samples

Fourier-Transform Infrared (FTIR) Spectroscopy was carried out using a JASCO FTIR-4100 spectrometer. In a typical procedure, the dried rubber was dissolved in chloroform (1% *w/v*) and stirred for 24 h. The obtained solution was cast and dried on a germanium (Ge) prism to get a thin film. The cast film attached to the Ge prism was then inserted into the spectrometer and measured at a resolution of 4 cm<sup>-1</sup> with 100 scans to analyze the functional group of samples.

<sup>1</sup>H-nuclear magnetic resonance (<sup>1</sup>H-NMR) spectroscopy was recorded on BRUKER 500 UltraShield<sup>™</sup>. 0.3–0.4% *w/v* of dried rubber was dissolved in *d*-chloroform (*d*-CDCl<sub>3</sub>). Then, the sample was subjected to a <sup>1</sup>H-NMR instrument.

Gel permeation chromatography (GPC) was used to determine the MW and molecular-weight distribution (MWD). The dried rubber was firstly dissolved in THF to make a solution with a concentration of 0.05% *w/v*. The solution was filtered through a 0.45 μm nylon-membrane syringe filter to remove impurities contaminating the solution. After that, 100 μL of the solution was injected into the JASCO-Borwin<sup>®</sup> GPC set-up equipped with RI (Jasco RI 1530) detectors using THF as an eluent at 35 °C, with a flow rate of 0.5 mL min<sup>-1</sup>. A column set was employed consisting of three sets of 300 × 8 mm columns in which the exclusion limits of a column packed with polystyrene-divinylbenzene gels of narrow

particle size distribution were  $4 \times 10^5$ ,  $5 \times 10^6$ , and  $2 \times 10^8$ . MWD was calculated based on polyisoprene standards.

### 3. Results and Discussion

#### 3.1. Characterization of TiO<sub>2</sub> Powder

The crystallinity of TiO<sub>2</sub> powder was preliminarily investigated. The clear diffraction peak in the X-ray diffraction (XRD) pattern was observed at  $2\theta$  of  $25.4^\circ$ , corresponding to the (101) plane of anatase, as shown in Figure 2. Other anatase peaks were observed at  $2\theta$  of the  $37.9^\circ$  (004),  $48.1^\circ$  (200),  $54.1^\circ$  (105), and  $55.4^\circ$  (211) planes. Moreover, the rutile peaks were also observed at  $2\theta$  of the  $27.5^\circ$  (110),  $36.1^\circ$  (101),  $41.4^\circ$  (111), and  $56.8^\circ$  (220) planes. This result indicated that P25-TiO<sub>2</sub> powder consisted of anatase and rutile phases. Hurum et al. proposed that the mixed-phase of anatase and rutile enhanced the photocatalytic activity of TiO<sub>2</sub> powder compared with the pure phase, since the rutile  $e^-$  was scavenged and the  $e^-$ - $h^+$  recombination was also hindered [19].

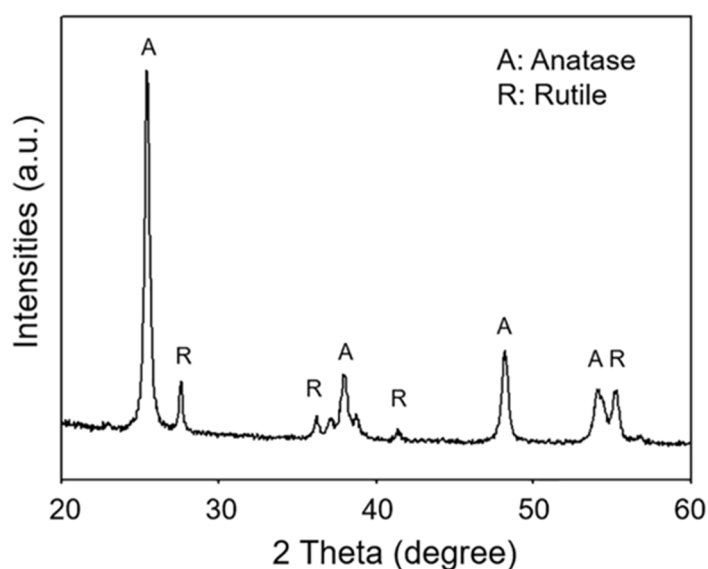
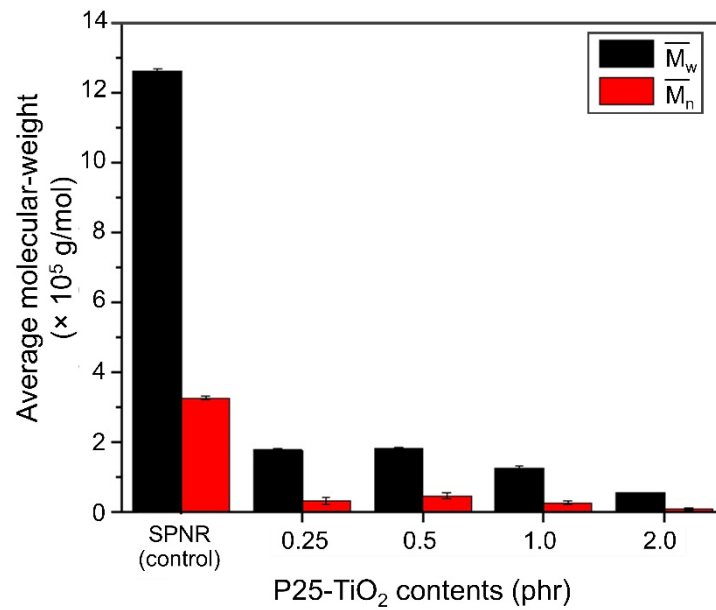


Figure 2. XRD pattern of P25-TiO<sub>2</sub> powder.

To examine the optimum condition for the FLNR latex preparation, the effect of TiO<sub>2</sub> powder content, H<sub>2</sub>O<sub>2</sub> concentration, and UVC-irradiation time were studied. The functional groups present on the rubber chains and the change in  $\bar{M}_n$  and  $\bar{M}_w$  before and after functionalization, including the chemical structure of the FLNR, were also investigated.

#### 3.2. Effect of the TiO<sub>2</sub> Powder Content on the MW and the Structure of SPNR and FLNR

In order that the UVC light can pass through the latex mixture efficiently, leading to an adequate energy for activating the TiO<sub>2</sub> powder, the low content of TiO<sub>2</sub> powder was varied between 0 and 2.0 phr. Figure 3 shows the  $\bar{M}_n$  and  $\bar{M}_w$  of SPNR and the samples obtained from the functionalization using different TiO<sub>2</sub> contents in the presence of 20%  $w/w$  H<sub>2</sub>O<sub>2</sub> under 5 h of UVC-irradiation. It was found that  $\bar{M}_n$  and  $\bar{M}_w$  dramatically decreased when the TiO<sub>2</sub> powder was incorporated, and it gradually decreased with an increase of TiO<sub>2</sub> content. At 2.0 phr of TiO<sub>2</sub> powder,  $\bar{M}_n$  and  $\bar{M}_w$  dropped to their lowest levels, which were about  $0.6 \times 10^5$  and  $0.1 \times 10^5$   $g\ mol^{-1}$ , respectively. However, the higher possible reactive site on the NR particles' surface is difficult to control for different NR chain lengths. It is reasonable to presume that shorter chains have a higher possibility of being broken down into a large number of low-MW NRs, resulting in the broadening of MWD after the degradation process. The MWD of the SPNR latex samples is shown in Figure 4, indicating the unimodal distribution for all samples.



**Figure 3.** The average MW of SPNR and samples prepared by introducing various TiO<sub>2</sub> powder contents in the presence of 20% *w/w* H<sub>2</sub>O<sub>2</sub> after UVC-irradiation for 5 h.

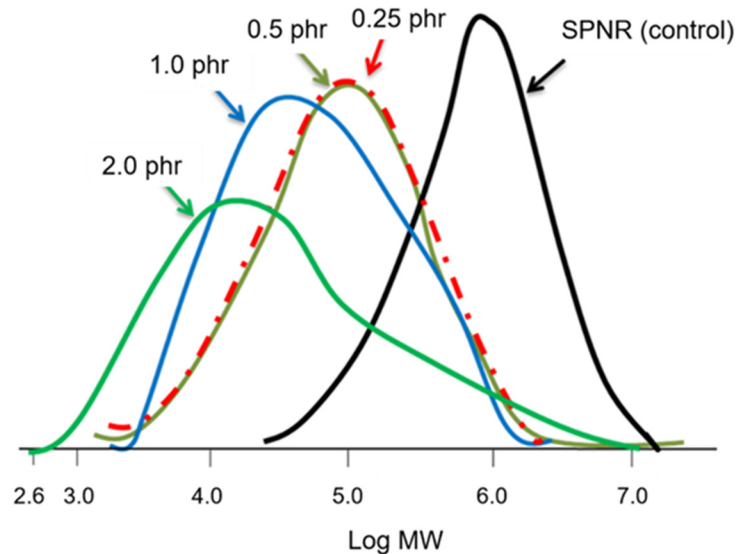


**Figure 4.** MWD of SPNR latex samples using H<sub>2</sub>O<sub>2</sub> 20% *w/w* with various TiO<sub>2</sub> powder contents under UVC-irradiation for 5 h.

The functional groups on rubber chains were observed by FTIR spectroscopy. FTIR spectra of SPNR and the samples are shown in Figure 5. The important characteristic bands for NR appear around 1664 and 836 cm<sup>-1</sup>, assigned to the C=C stretching and =C-H deformation, respectively [20]. The new transmittance peak around 3440 cm<sup>-1</sup>, corresponding to the -OH group, was observed in the sample prepared in the system containing TiO<sub>2</sub> powder, and the peak intensity increased with the increase of TiO<sub>2</sub> content from 0 to 2.0 phr. This suggests that TiO<sub>2</sub> accelerates the photochemical degradation of SPNR latex through the photocatalysis on the TiO<sub>2</sub> surface. The higher the amount of TiO<sub>2</sub> powder, the higher the -OH groups from the oxidation phenomena. The generated OH- attached to the broken points of polyisoprene chains, which shortened during the reaction, confirmed the decrease in the average MW given in Figure 3.

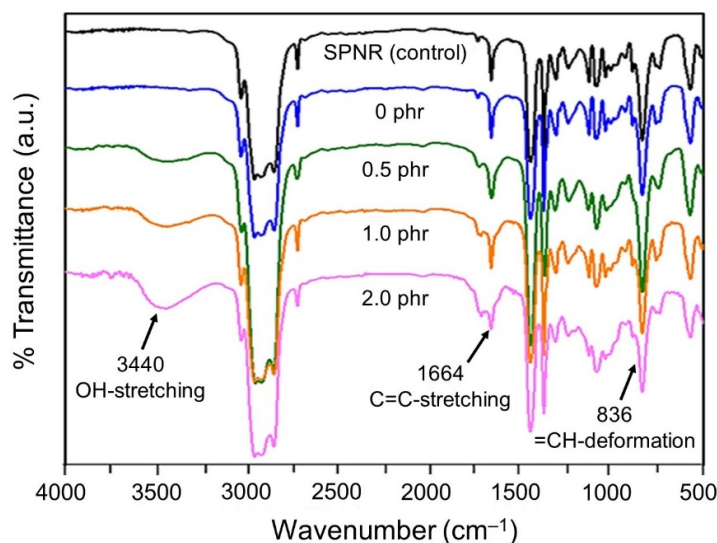


**Figure 5.** FTIR spectra of SPNR and samples with various  $\text{TiO}_2$  contents in the presence of 20%  $w/w$   $\text{H}_2\text{O}_2$  after UVC-irradiation for 5 h.

### 3.3. Effect of $\text{H}_2\text{O}_2$ Content on the MW and the Structure of SPNR and FLNR

The  $\bar{M}_w$  and  $\bar{M}_n$  of SPNR and the samples prepared by introducing 2.0 phr of  $\text{TiO}_2$  powder with different  $\text{H}_2\text{O}_2$  concentrations under UVC-irradiation are shown in Figure 6. It is clear that  $\bar{M}_n$  and  $\bar{M}_w$  slightly decreased in the presence of  $\text{TiO}_2$  without  $\text{H}_2\text{O}_2$ , but drastically decreased when the  $\text{H}_2\text{O}_2$  was introduced. Moreover, both the  $\bar{M}_n$  and  $\bar{M}_w$  of the samples decreased with an increase of the  $\text{H}_2\text{O}_2$  concentration.

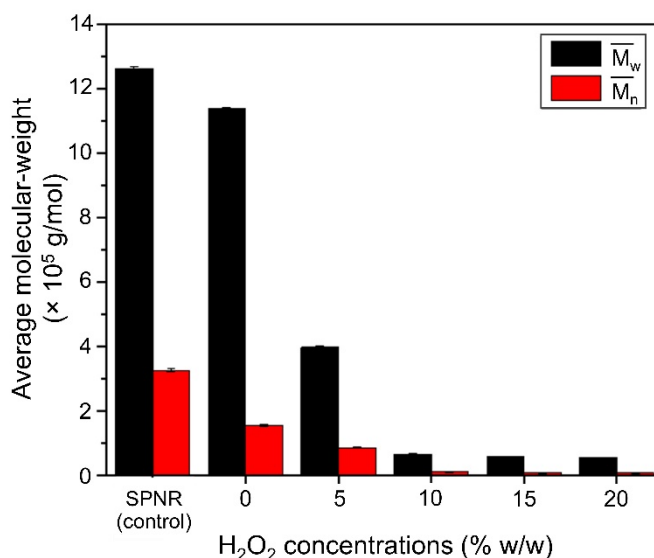


**Figure 6.** The average MW of SPNR and the samples prepared by introducing 2.0 phr of  $\text{TiO}_2$  powder with various  $\text{H}_2\text{O}_2$  concentrations after UVC-irradiation for 5 h.

Given this result, we assumed that the average MW of the samples decreased because many  $\text{OH}\cdot$  took place in the system, which was generated from both  $\text{TiO}_2$  photocatalysis and the degradation of  $\text{H}_2\text{O}_2$  under UVC-irradiation [21]. The functional groups on SPNR and the samples prepared by introducing 2.0 phr of  $\text{TiO}_2$  powder at different  $\text{H}_2\text{O}_2$  concentrations are shown in Figure 7. The  $-\text{OH}$  group at around  $3440\text{ cm}^{-1}$  was obviously observed when  $\text{H}_2\text{O}_2$  was introduced in the system, and it increased with the increasing of  $\text{H}_2\text{O}_2$  concentration. The highest  $-\text{OH}$  intensity was observed in the sample containing 20%  $w/w$   $\text{H}_2\text{O}_2$ . This suggests that the increase of the  $-\text{OH}$  group resulted from the dissociation

of  $\text{H}_2\text{O}_2$  under UVC, apart from the oxidation of rubber via the photocatalytic reaction on the  $\text{TiO}_2$  surface. These observations were correlated with the result shown in Figure 6.

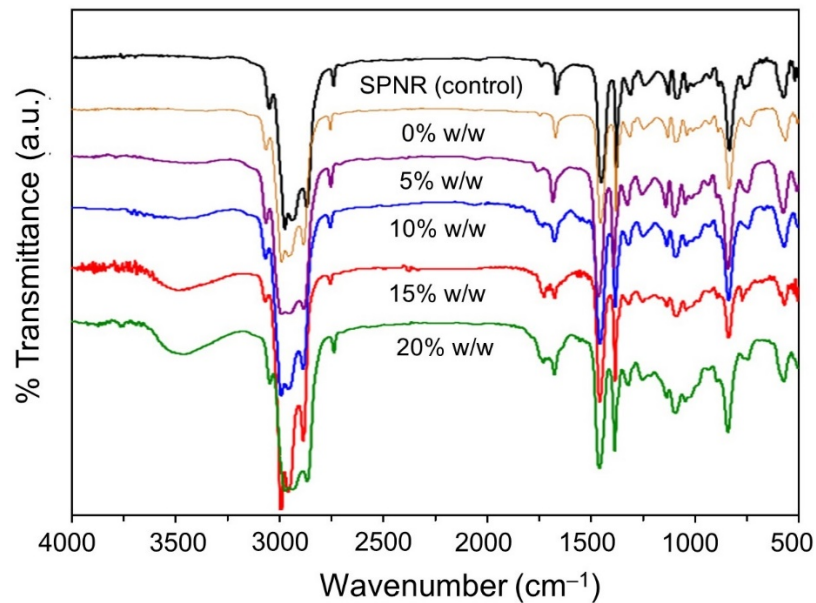


**Figure 7.** FTIR spectra of SPNR and the samples prepared by introducing 2.0 phr of  $\text{TiO}_2$  powder with various  $\text{H}_2\text{O}_2$  concentrations after UVC-irradiation for 5 h.

#### 3.4. Effect of UVC-Irradiation Time on the SPNR and FLNR Structures

The FTIR spectra of SPNR and the samples prepared from different UVC-irradiation time containing 2.0 phr  $\text{TiO}_2$  powder and 20% *w/w*  $\text{H}_2\text{O}_2$  are exhibited in Figure 8. The transmittance peak at around  $3440\text{ cm}^{-1}$ , corresponding to  $-\text{OH}$ , increases with the increasing time of irradiation and presents the highest intensity under irradiation for 5 h. However, the  $-\text{OH}$  peak was found to decrease after UVC-irradiation for 6 h. This might be due to the occurrence of some unfavorable processes: (i) excess amounts of OH and other reactive radicals generated from the direct decomposition of  $\text{H}_2\text{O}_2$  by UVC light and the formation of radicals on the  $\text{TiO}_2$  surface, leading to a low quantum efficiency for this method, and (ii) the recombination of  $\text{h}^+$  and  $\text{e}^-$  during the photocatalytic degradation process.

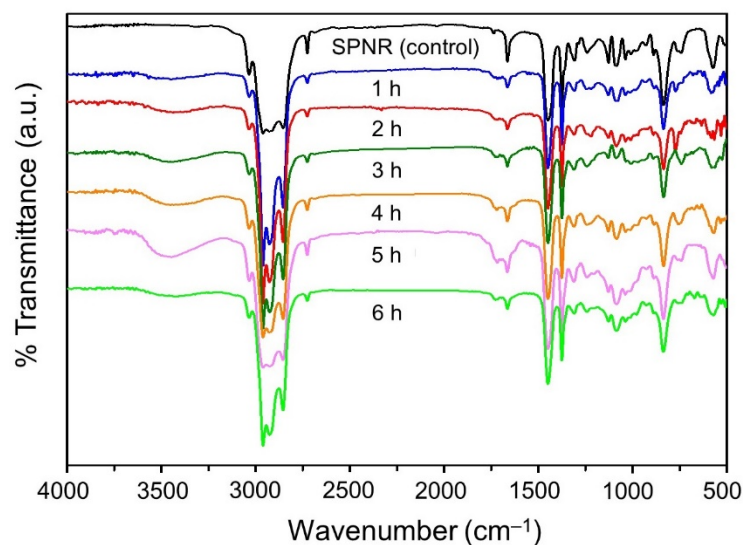


**Figure 8.** FTIR spectra of SPNR and the samples prepared by introducing 2.0 phr of  $\text{TiO}_2$  powder in the presence of 20% *w/w*  $\text{H}_2\text{O}_2$  after various UVC-irradiation times.

The microstructure of FLNR was confirmed by the  $^1\text{H-NMR}$  spectrum, as shown in Figure 9. The proton peaks of NR at  $\delta = 1.25$ , 2.00, and 5.12 ppm were assigned to  $-\text{CH}_3$ ,  $-\text{CH}_2-$ , and  $-\text{C}=\text{CH}$ , respectively [22]. In addition, the additional small peaks at 3.49 and 3.74 ppm were also detected, corresponding to  $-\text{OH}$  and  $>\text{CH}-\text{OH}$ , respectively. These observations implied that some  $-\text{OH}$  groups were present on the FLNR chain-ends [23,24]. The proposed structure is indicated in Figure 9.

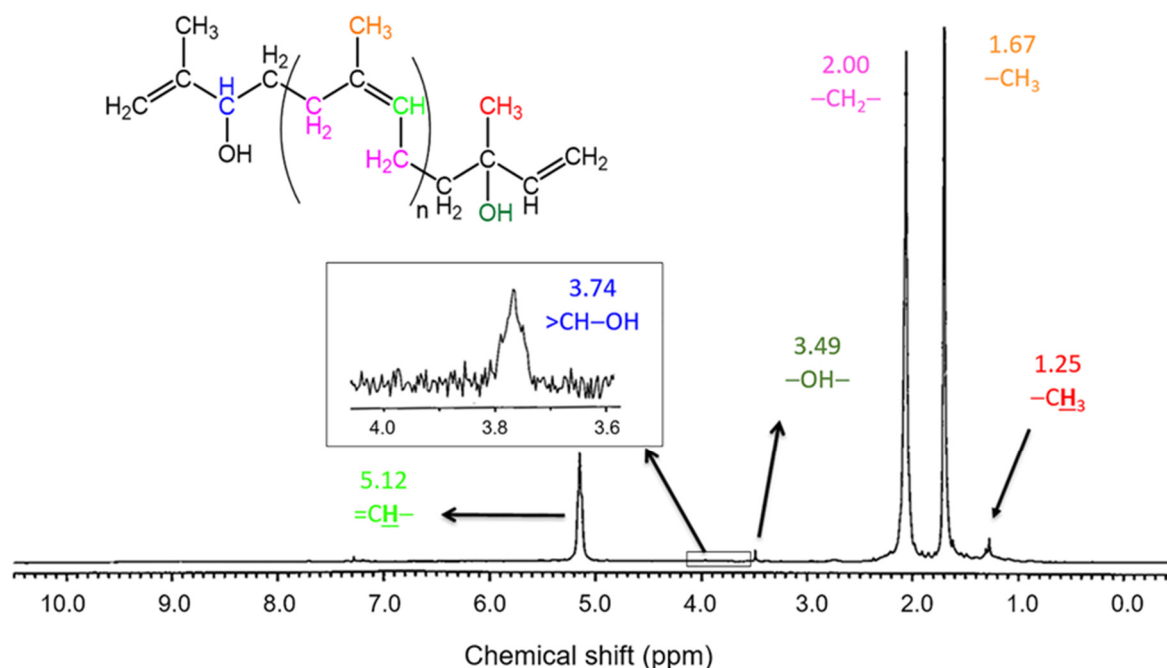


**Figure 9.**  $^1\text{H-NMR}$  spectrum of FLNR prepared by SPNR in the presence of 2.0 phr of  $\text{TiO}_2$  powder and 20%  $w/w$   $\text{H}_2\text{O}_2$  under UVC-irradiation for 5 h.

#### 4. Conclusions

The functionalized low-molecular-weight NR (FLNR) latex with a terminated hydroxyl group was successfully prepared by the photochemical degradation process of saponified NR (SPNR) latex in the presence of  $\text{H}_2\text{O}_2$  using P25- $\text{TiO}_2$  powder as a photocatalyst under UVC-irradiation. The elimination of the mixed layer of lipids and proteins surrounding the NR particles' surface by the saponification was profitable on the degradation mechanism on NR chains due to the enhancement of reagents attachment. The contents of  $\text{TiO}_2$  powder and  $\text{H}_2\text{O}_2$  as well as UVC-irradiation time were found to affect the degradation of NR. After 80W UVC-irradiation for 5 h in the presence of 20%  $w/w$   $\text{H}_2\text{O}_2$  and 2.0 phr of P25- $\text{TiO}_2$  powder, the weight average MW of SPNR dramatically decreased from  $12.6 \times 10^5$  to  $0.6 \times 10^5 \text{ gmol}^{-1}$ , while the average MW decreased from  $3.3 \times 10^5$  to  $0.1 \times 10^5 \text{ gmol}^{-1}$ . In addition, the  $-\text{OH}$  groups were also clearly observed on the NR chains, and their contents were found to be increased with increasing  $\text{TiO}_2$  and  $\text{H}_2\text{O}_2$  contents and UV irradiation time. The presence of  $-\text{OH}$  groups is thought to be caused by the attachment of  $\text{OH}\cdot$  on the broken points of polyisoprene chains—which were shortened during the reaction, due to the  $\text{H}_2\text{O}_2$  dissociation—and the photocatalysis on the  $\text{TiO}_2$  surface. It can be concluded that the  $\text{H}_2\text{O}_2/\text{P25-TiO}_2$  powder/UVC-irradiation system is an efficient, clean, and economical method for the preparation of FLNR latex.

**Author Contributions:** Conceptualization, J.S. and P.R.; methodology, J.S., S.N. and P.R.; formal analysis, S.N.; investigation, S.N.; data curation, J.S., S.N.; writing: original draft preparation, J.S., S.N.; writing: review and editing, J.S., A.N. and P.R.; visualization, S.N.; supervision, J.S.; project administration, J.S.; funding acquisition, J.S. All authors have read and agreed to the published version of the manuscript.

**Funding:** This research was funded by the Thailand Science Research and Innovation (former Thailand Research Fund), the National Research Council of Thailand (NRCT), and Mahidol University, grant number NRCTS-RSA63015-09.

**Institutional Review Board Statement:** Not applicable.

**Informed Consent Statement:** Not applicable.

**Data Availability Statement:** The data presented in this study are available on request from the corresponding author.

**Acknowledgments:** This work was supported by the Thailand Science Research and Innovation (former Thailand Research Fund), the National Research Council of Thailand (NRCT) and Mahidol University. The authors also gratefully acknowledge Mahidol University and the Center of Excellence for Innovation in Chemistry (PERCH-CIC), Ministry of Higher Education, Science, Research and Innovation. Sincere appreciation is extended to the Thai Rubber Latex Group Public Co., Ltd., for supplying the NR latex.

**Conflicts of Interest:** The authors declare no conflict of interest. The funders had no role in the design of the study; in the collection, analyses, or interpretation of data; in the writing of the manuscript, or in the decision to publish the results.

## References

1. Tarachiwin, L.; Sakdapipanich, J.; Ute, K.; Kitayama, T.; Tanaka, Y. Structural Characterization of  $\alpha$ -Terminal Group of Natural Rubber. 2. Decomposition of Branch-Points by Phospholipase and Chemical Treatments. *Biomacromolecules* **2005**, *6*, 1858–1863. [[CrossRef](#)]
2. Lake, G.J.; Samsuri, A.; Teo, S.C.; Vaja, J. Time-Dependent Fracture in Vulcanized Elastomers. *Polymer* **1991**, *32*, 2963–2975. [[CrossRef](#)]
3. Srilathakutty, R.; John, N.; Joseph, R.; George, K.E. Use of Amine Terminated Liquid Natural Rubber as a Plasticiser in Filled NR and NBR Compounds. *Int. J. Polym. Mater. Polym. Biomater.* **1996**, *32*, 235–246. [[CrossRef](#)]
4. Mounir, A.; Darwish, N.A.; Shehata, A. Effect of Maleic Anhydride and Liquid Natural Rubber as Compatibilizers on the Mechanical Properties and Impact Resistance of the NR-NBR Blend. *Polym. Adv. Technol.* **2004**, *15*, 209–213. [[CrossRef](#)]
5. Dahlan, H.M.; Zaman, M.D.K.; Ibrahim, A. Liquid Natural Rubber (LNR) as a Compatibiliser in NR/LLDPE Blends—II: The Effects of Electron-beam (EB) Irradiation. *Radiat. Phys. Chem.* **2002**, *64*, 429–436. [[CrossRef](#)]
6. Phetphaisit, C.W.; Bumeer, R.; Namahoot, J.; Ruamcharoen, J.; Ruamcharoen, P. Polyurethane Polyester Elastomer: Innovative Environmental Friendly Wood Adhesive from Modified PETs and Hydroxyl Liquid Natural Rubber Polyols. *Int. J. Adhes. Adhes.* **2013**, *41*, 127–131. [[CrossRef](#)]
7. Kaenhin, L.; Klinpituksa, P.; Rungvichaniwat, A.; Pilard, J.-F. Waterborne Polyurethane: Effect of Functional Groups in Aromatic Isocyanate and the Chain Length of Hydroxyl Terminated Natural Rubber. *Adv. Mater. Res.* **2012**, *415–417*, 2032–2035. [[CrossRef](#)]
8. Saetung, A.; Kaenhin, L.; Klinpituksa, P.; Rungvichaniwat, A.; Tulyapitak, T.; Munleh, S.; Campistrion, I.; Pilard, J.-F. Synthesis, Characteristic, and Properties of Waterborne Polyurethane Based on Natural Rubber. *J. Appl. Polym. Sci.* **2012**, *124*, 2742–2752. [[CrossRef](#)]
9. Kébir, N.; Campistrion, I.; Laguerre, A.; Pilard, J.-F.; Bunel, C. New Crosslinked Polyurethane Elastomers with Various Physical Properties from Natural Rubber Derivatives. *J. Appl. Polym. Sci.* **2011**, *122*, 1677–1687. [[CrossRef](#)]
10. Ly, P.H. Reinforcement of Natural Rubber from Hydroxyl-Terminated Liquid Natural Rubber Grafted Carbon Black. I. Grafting of Acyl Chloride Capped Liquid Natural Rubber onto Carbon Black. *J. Macromol. Sci. Part A Pure Appl. Chem.* **1996**, *33*, 1931–1937. [[CrossRef](#)]
11. Isa, S.Z.; Yahya, R.; Hassan, A.; Tahir, M. The Influence of Temperature and Reaction Time in the Degradation of Natural Rubber Latex. *Malays. J. Anal. Sci.* **2007**, *11*, 42–47.
12. Ibrahim, S.; Daik, R.; Abdullah, I. Functionalization of Liquid Natural Rubber via Oxidative Degradation of Natural Rubber. *Polymers* **2014**, *6*, 2928–2941. [[CrossRef](#)]
13. Ibrahim, S.; Sreekantan, S.; Tan, K.S.; Nor, Z.M.; Ismail, H. Preparation and Characterization of Low-Molecular-Weight Natural Rubber Latex via Photodegradation Catalyzed by Nano TiO<sub>2</sub>. *Polymers* **2018**, *10*, 1216. [[CrossRef](#)]
14. Ravindran, T.; Nayar, M.R.G.; Francis, D.J. Production of Hydroxyl-Terminated Liquid Natural Rubber—Mechanism of Photochemical Depolymerization and Hydroxylation. *J. Appl. Polym. Sci.* **1988**, *35*, 1227–1239. [[CrossRef](#)]
15. Nijpanich, S.; Nimpai boon, A.; Sakdapipanich, J. Functionalization of Styrene-Butadiene Rubber and Skim Latex by Photocatalytic Reaction Using Nanometric TiO<sub>2</sub> Film as a Photocatalyst. *Key Eng. Mater.* **2015**, *659*, 409–413. [[CrossRef](#)]
16. Negishi, N.; Takeuchi, K.; Ibusuki, T. The Surface Structure of Titanium Dioxide Thin Film Photocatalyst. *Appl. Surf. Sci.* **1997**, *121–122*, 417–420. [[CrossRef](#)]
17. Nawamawat, K.; Sakdapipanich, J.T.; Ho, C.C.; Ma, Y.; Song, J.; Vancso, J.G. Surface Nanostructure of *Hevea brasiliensis* Natural Rubber Latex Particles. *Colloids Surf. A* **2011**, *390*, 157–166. [[CrossRef](#)]

18. Yunyongwattanakorn, J.; Tanaka, Y.; Sakdapipanich, J.; Wongsasutthikul, V. Highly-Purified Natural Rubber by Saponification of Latex: Analysis of Residual Proteins in Saponified Natural Rubber. *Rubber Chem. Technol.* **2008**, *81*, 121–137. [[CrossRef](#)]
19. Hurum, D.C.; Agrios, A.G.; Gray, K.A.; Rajh, T.; Thurnauer, M.C. Explaining the Enhanced Photocatalytic Activity of Degussa P25 Mixed-Phase TiO<sub>2</sub> Using EPR. *J. Phys. Chem. B* **2003**, *107*, 4545–4549. [[CrossRef](#)]
20. Dafader, N.C.; Haque, M.E.; Akhtar, F.; Ahmad, M.U. Study on Grafting of Different Types of Acrylic Monomers onto Natural Rubber by  $\gamma$ -rays. *Radiat. Phys. Chem.* **2006**, *75*, 168–172. [[CrossRef](#)]
21. Alaton, I.A.; Balcioglu, I.A.; Bahnemann, D.W. Advanced Oxidation of a Reactive Dyebath Effluent: Comparison of O<sub>3</sub>, H<sub>2</sub>O<sub>2</sub>/UV-C and TiO<sub>2</sub>/UV-A Processes. *Water Res.* **2002**, *36*, 1143–1154. [[CrossRef](#)]
22. Phinyocheep, P.; Phetphaisit, C.W.; Derouet, D.; Campistron, I.; Brosse, J.C. Chemical Degradation of Epoxidized Natural Rubber Using Periodic acid: Preparation of Epoxidized Liquid Natural Rubber. *J. Appl. Polym. Sci.* **2005**, *95*, 6–15. [[CrossRef](#)]
23. Sakdapipanich, I.; Nawamawat, K. Effect of treatment of skim natural rubber latex on properties of pressure-sensitive adhesive tapes. *Kauchuk i Rezina* **2005**, *5*, 9–11.
24. Saetung, A.; Rungvichaniwat, A.; Campistron, I.; Klinpituksa, P.; Laguerre, A.; Phinyocheep, P.; Doutres, O.; Pilard, J.-F. Preparation and Physico-Mechanical, Thermal and Acoustic Properties of Flexible Polyurethane Foams Based on Hydroxytelechelic Natural Rubber. *J. Appl. Polym. Sci.* **2010**, *117*, 828–837. [[CrossRef](#)]